Journal of Radiation Research, 2013, 54, 950–956
doi: 10.1093/jrr/rrt017 Advance Access Publication 5 April 2013

Geometrical differences in gross target volumes between 3DCT and 4DCT imaging in radiotherapy for non-small-cell lung cancer

Fengxing LI[1], Jianbin LI[1,*], Yingjie ZHANG[1], Min XU[1], Dongping SHANG[2], Tingyong FAN[1], Tonghai LIU[2] and Qian SHAO[1]

[1]Department of Radiation Oncology, Shandong Cancer Hospital and Institute, Jinan 250117, China
[2]Big Bore CT Room, Shandong Cancer Hospital and Institute, Jinan 250117, China
*Corresponding author. Department of Radiation Oncology, Shandong Cancer Hospital and Institute, Jinan 250117, China. Tel: +86-531-6762-6131; Fax: +86-531-6762-6130; Email: lijianbin@msn.com

(Received 3 April 2012; revised 6 February 2013; accepted 8 February 2013)

The aim of this study was to explore the characteristic of 3DCT scanning phases and estimate the comparative amount of respiration motion information included in 3DCT and 4DCT by comparing the volumetric and positional difference between the volumes from 3DCT and 4DCT for the radiotherapy of non-small-cell lung cancer (NSCLC). A total of 28 patients with NSCLC sequentially underwent 3DCT and 4DCT simulation scans of the thorax during free breathing. The 4DCT images with respiratory signal data were reconstructed and sorted into 10 phases throughout a respiratory cycle. GTV-3D from 3DCT, GTV-0%, GTV-20%, GTV-50% and GTV-70% from end-inspiration, mid-expiration, end-expiration and mid-inspiration of 4DCT, and the internal GTV (IGTV-10) from the fused phase of 4DCT were delineated based on the 50% phase image, respectively. The differences in the position, size, matching index (MI) and degree of inclusion (DI) for different volumes were evaluated. The variation in the centroid shifts of GTV-0% and GTV-3D, GTV-20% and GTV-3D, GTV-50% and GTV-3D, and GTV-90% and GTV-3D in the 3D direction was not significant ($P = 0.990$). The size ratios of GTV-0%, GTV-20%, GTV-50%, GTV-70% and IGTV-10 to GTV-3D were 0.94 ± 0.18, 0.95 ± 0.18, 0.98 ± 0.15, 1.00 ± 0.18 and 1.60 ± 0.55, respectively. DIs of GTV-3D in IGTV-10, and IGTV-10 in GTV-3D were 0.88 ± 0.14 and 0.59 ± 0.16 ($P < 0.001$). The 3DCT scanning phases are irregular. The CTV-to-ITV expansion should be isotropic when defining the ITV on the 3DCT. The internal GTV derived from 4DCT cannot completely include the GTV from 3DCT. An additional margin may be required when defining the ITV-based 4DCT.

Keywords: non-small-cell lung cancer; 4DCT; 3DCT; gross tumor volume; volume comparison

INTRODUCTION

Modern radiotherapy has moved into the new era of high precision radiotherapy. High precision radiation therapy (HPRT) relies heavily on high-fidelity medical imaging (HFMI) [1]. However, conventional 3DCT cannot be considered HFMI in the radiotherapy of non-small-cell lung cancer (NSCLC) due to respiration-induced tumor motion. Scanning of tumors during respiratory motion with modern fast 3DCT has a high potential of introducing significant artifacts [2, 3], which may have a great impact on the accuracy of target volume delineation and dose calculation. In addition, temporal images acquired during 3DCT scanning cannot completely encompass respiration-induced tumor motion.

Deep inspiration breath hold (DIBH) and respiratory gating techniques effectively reduce respiration-induced organ motion. They not only reduce motion artifacts often seen on fast 3DCT [4, 5], but also reduce the margin accounting for respiratory motion [6]. However, breath-hold scans may not be tolerated by patients with poor lung functionality [7], and the extreme images acquired by the technique may not represent the extreme phases of free respiration. These issues limit the usefulness of the DIBH technique. Slow CT imaging can almost incorporate an entire breathing cycle in one imaging section, and then capture tumor mobility information to generate individual internal target volumes (ITVs) [8–10]. However, the slow CT image of a moving tumor usually shows significant

respiratory motion artifacts [11]. So it is difficult to obtain accurate tumor/organ shapes using the slow CT technique.

Recently, 4DCT has been widely used for the simulation of lung cancer. It provides 'instant' capture of the target volume corresponding to different respiratory phases throughout a respiratory cycle. Respiratory motion artifacts can be mitigated by 4DCT that accounts for respiratory motion [12]. Moreover, most patients can tolerate 4DCT scanning, because it is performed during free breathing.

The temporal image acquired during the conventional axial 3DCT scan may include some respiration motion information, but it has been difficult to evaluate how much motion information the 3DCT encompasses. The 4DCT is a reliable and effective tool for assessing tumor motion [13, 14]. Many researchers have compared 3DCT volumes with 4DCT volumes [7, 15, 16], however, most of these have focused on comparing 3D volumes with 4D composite volumes [7, 15]. In this article, we have not only analyzed the volumetric and positional differences of the GTV on the axial 3DCT, and the internal GTV (IGTV) derived from 10 phases of 4DCT, but also compared the 3DCT-based GTV with the GTVs from different phases of 4DCT.

The three aims of this study were: (i) to explore the characteristic of 3DCT scanning phases by assessing whether there is an intrinsic correlation between conventional 3DCT and a certain phase of 4DCT; (ii) to estimate the comparative amount of respiration motion information included in 3DCT and 4DCT by quantifying the volumetric difference and inclusion relation between the GTV from 3DCT and the IGTV from 10 phases of 4DCT; (iii) to analyze the volumetric variation in GTVs derived from the 10 phases of the 4DCT.

MATERIALS AND METHODS

Patient characteristics

A total of 28 patients with peripheral NSCLC underwent 4DCT simulation for treatment planning between September 2009 and July 2010 in Shandong Cancer Hospital and Institute. Pathology demonstrated adenocarcinoma in 21 patients, squamous cell carcinoma in 6 patients, and adenosquamous carcinoma in 1 patient. The patients included 19 men and 9 women, and had a median age of 60 (range, 39–80). The T stage, according to the TNM classification of AJCC (7th edn, 2009), was classified as T1 in 17 patients, T2 in 7 patients and T3 in 4 patients. The patients were divided in two groups: those with lesions located in the upper lobe (16 patients) belonging to Group A, while those with lesions located in the middle lobe (3 patients) or in the lower lobe (9 patients) were combined to make up Group B. All patients provided written informed consent prior to treatment planning.

CT simulation and image acquisition

Vacuum bags were used to immobilize all patients in the supine position with arms raised above the head. For each person, an axial 3DCT scan of the thoracic region was performed, followed by a 4DCT scan during uncoached free breathing on a 16-slice CT scanner (Philips Brilliance Bores CT). For 3DCT scanning, each scan (360° rotation) took 1 s to acquire, followed by a 1.8 s dead time, with a 2.4-cm coverage. The whole axial 3DCT scanning procedure for the thoracic region took about 30 s. The 4D acquisition protocol has been described in our previous study [17]. The 4DCT images were sorted into 10 bins according to the phase of the breathing signal, with 0% corresponding to end-inhalation and 50% corresponding to end-exhalation. Both the 3DCT and 4DCT images were reconstructed using a thickness of 3 mm, and then transferred to the Eclipse treatment planning system (Varian Eclipse 8.6).

GTVs delineation

GTVs were manually delineated on the 10 phases of the 4DCT images and the 3DCT image by a radiation oncologist using the lung window setting (window width: 1600 HU and window level: –600 HU) [18]. 'Partial volume effect' and 'partial projection effect for moving objects' on 3DCT and 4DCT manifest as blurring of object boundaries. The entire blurred extent of the tumor was delineated as the GTV. Because the 3DCT images and the 4DCT images for a given person were produced during the same imaging session, Eclipse considers the images as being registered with each other. Firstly, GTV-0%, GTV-20% and GTV-70% derived from end-inspiration (0% phase), mid-expiration (20% phase) and mid-inspiration (70% phase) images were copied onto the end-expiration (50% phase) image (Fig. 1), then, the IGTV-10, encompassing all of these 4DCT-based GTVs, was produced on the end-expiration image by merging the 10 GTVs derived from all phases of 4DCT; lastly, the GTV-3D, derived from 3DCT, was copied onto the end-expiration image.

Volumes comparison

Volume, position, matching index (MI) and degree of inclusion (DI) between the 4D volumes (GTV-0%, GTV-20%, GTV-50%, GTV-70% and IGTV-10) and the 3D volume (GTV-3D) were compared, respectively. The position for each tumor was expressed using the x (left-right, LR), y (anterior-posterior, AP) and z (cranial-caudal, CC) coordinates of the center of mass for each bin for 4DCT. Then, the intra-fractional motion range of the center of mass in each coordinate was obtained. The 3D motion vector of the center of mass was calculated according to the formula as follows:

$$\text{Vector} = \sqrt{\text{LR}^2 + \text{AP}^2 + \text{CC}^2}.$$

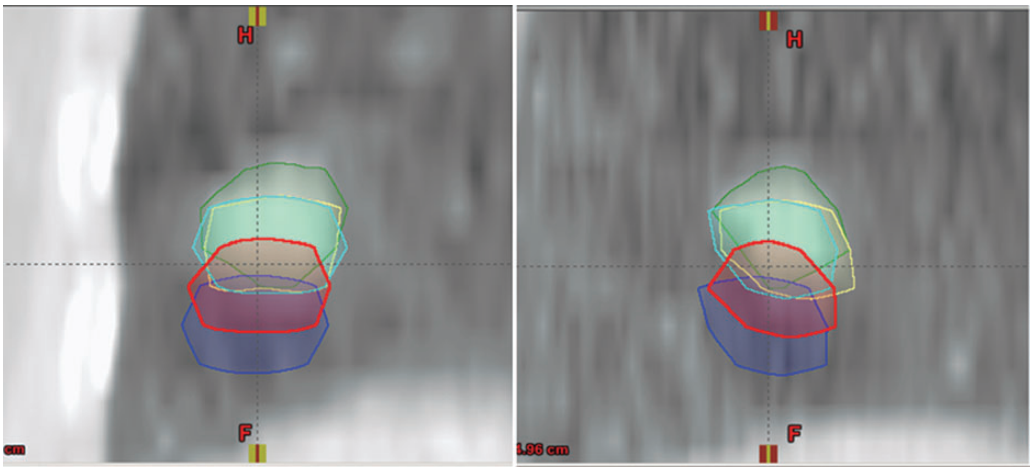

Fig. 1. Example of the GTV-3D (red segment), GTV-0% (blue segment), GTV-20% (yellow segment), GTV-50% (dark green) and GTV-70% (cyan segment) delineated on the 50% phase of the 4DCT in coronal (left), and sagittal (right) planes for one patient (Patient 6). The tumor motion vector was 1.37 cm.

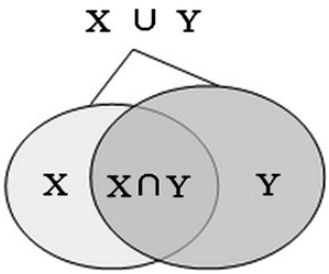

Fig. 2. Schematic illustration of the intersection of X with Y (X ∩ Y) and the union of X with Y (X ∪ Y).

The matching index of volume X and Y [MI (X, Y)] was computed according to the method used by Ezhil *et al.* [19], i.e. defined as the ratio of the intersection of X with Y to the union of X and Y (Fig. 2). The MI integrates the size, space location and shape features of two volumes, and represents their degree of similarity. The maximum value of MI is 1 if the two volumes are identical, and the minimum value is 0 if the volumes are completely non-overlapping. The formula is as follows:

$$\mathrm{MI}(\mathrm{X},\ \mathrm{Y}) = \frac{\mathrm{X} \cap \mathrm{Y}}{\mathrm{X} \cup \mathrm{Y}}.$$

Although MI is a good measure of how well the shape of any two volumes matches each other, it cannot quantify the percentage of one volume included by another volume. The definition of DI of volume X in volume Y [DI (X in Y)] is the percentage of the intersection of volume X and Y in volume X [17]. The DI can represent the percentage of one volume included by another volume, while 1-DI can represent the percentage of one volume not included by another volume. The formula is as follows:

$$\mathrm{DI}(\mathrm{X\ in\ Y}) = \frac{\mathrm{X} \cap \mathrm{Y}}{\mathrm{X}}.$$

Statistical analysis

Statistical analysis was performed using the SPSS software package (SPSS 16.0 for Windows). A one-way ANOVA test was used to determine the variations in the centroid shifts and the MIs of GTV-3D and GTV-0%, GTV-3D and GTV-20%, GTV-3D and GTV-50%, and GTV-3D and GTV-70%. The paired t-test was used to determine paired data variables. The wilcoxon test was performed to test data for Group A and Group B variables. We used the Pearson correlation test to analyze for associations between GTV motion vectors and continuous variables (e.g. size, MI and DI). Values of $P < 0.05$ were regarded as significant for all the tests.

RESULTS

GTV volume and motion

The mean of the average size of GTVs from 10 phases for all patient were 7.96 ± 10.59 cm^3 (range, 0.32–37.08 cm^3). The mean of the standard deviation (SD) of GTVs from 10 phases for all patients was 0.51 ± 0.75 cm^3 (range, 0.02–3.4 cm^3). The mean coefficient of variation (SD/Mean) of GTVs was $8.76\% \pm 6.47\%$ (range, 1.94–23.73%). Figure 3 illustrates the tumor motion in the LR, AP, CC and 3D directions for each patient. The mean tumor motion amplitudes were 1.6 ± 1.0 mm, 2.1 ± 1.1 mm, 4.0 ± 3.9 mm and 5.2 ± 3.5 mm in the LR, AP, CC and 3D directions, respectively. The tumor motion in the LR, AP and CC directions were 1.4 ± 0.8 mm, 1.8 ± 1.0 mm and 1.8 ± 1.8 mm for Group A, and 1.8 ± 1.3 mm, 2.5 ± 1.1 mm and 6.9 ± 4.0 mm for Group B, respectively. The mean 3D motion vector was 3.2 ± 1.7 mm for Group A, and 8.0 ± 3.5 mm for Group B, with a significant statistical difference ($z = 0.667$, $P < 0.001$).

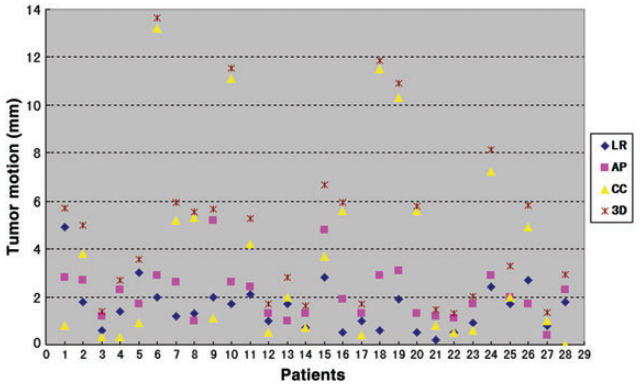

Fig. 3. The tumor motion in the left-right (LR), anterior-posterior (AP), cranial-caudal (CC) and three dimensional (3D) directions for each patient.

Centroid shifts of the volumes derived from 3DCT and 4DCT

Table 1 shows the centroid shifts in the LR, AP, CC and 3D directions of the 4D volumes and the 3D volume. Comparing the centroid shift of 4D volumes with that of the GTV-3D in a certain direction showed that the shift of GTV-50% and GTV-3D in the CC direction was largest (2.0 ± 1.9 mm), while the shift of GTV-50% and GTV-3D in the LR direction was smallest (-0.3 ± 1.1 mm). The centroid shift of IGTV-10 and GTV-3D (2.4 ± 1.4 mm) in the 3D direction was smaller than the shifts of GTV-0% and GTV-3D, GTV-20% and GTV-3D, GTV-50% and GTV-3D, and GTV-70% and GTV-3D (P = 0.05, 0.386, 0.034, and 0.003, respectively). The variation in the centroid shifts in the 3D direction of GTV-0% and GTV-3D, GTV-20% and GTV-3D, GTV-50% and GTV-3D, and GTV-70% and GTV-3D was not significant ($F = 0.037$, $P = 0.990$).

Volume variation

Figure 4 shows the 4D and 3D target volumes for all patients. The mean size of GTV-0%, GTV-20%, GTV-50%, and GTV-70% for all patients was 8.23 ± 11.17 cm^3, 7.95 ± 10.33 cm^3, 7.99 ± 10.36 cm^3, and 8.17 ± 10.35 cm^3, respectively. The volumetric variation was not significant among the four phases ($F = 0.005$, $P = 0.999$). The GTV-3D size (8.37 ± 11.41 cm^3) was smaller than IGTV-10 (11.83 ± 15.03 cm^3) ($P = 0.001$). Figure 5 displays the size ratio of the 4D volume to GTV-3D. The size ratios of GTV-0%, GTV-20%, GTV-50% and GTV-70% to GTV-3D were 0.94 ± 0.18, 0.95 ± 0.18, 0.98 ± 0.15 and 1.00 ± 0.18, respectively. The size ratio of IGTV-10 to GTV-3D was 1.60 ± 0.55, which showed a significant correlation to the motion vector ($r = 0.667$, $P < 0.001$). The median size ratio of IGTV-10 to GTV-3D for Group A and Group B were 1.34 and 1.67, respectively, with a significant difference ($P = 0.010$).

Table 1. The mean and range (absolute) of centroid shifts of the 4D volume and 3D volume in the left–right (LR), anterior–posterior (AP), cranial–caudal (CC) and three-dimensional (3D) directions

Volumes	LR (mm)	AP (mm)	CC (mm)	3D (mm)
GTV-0% – GTV-3D	–0.7 ± 1.1 (0.0–3.2)	1.0 ± 1.2 (0.0–2.9)	–1.2 ± 2.2 (0.1–5.0)	2.9 ± 1.4 (0.2–5.0)
GTV-20% – GTV-3D	–0.4 ± 0.9 (0.0–2.0)	0.6 ± 1.4 (0.0–3.1)	0.5 ± 2.3 (0.0–6.6)	2.4 ± 1.6 (0.2–7.3)
GTV-50% – GTV-3D	–0.3 ± 1.1 (0.0–3.3)	0.9 ± 1.9 (0.0–5.7)	2.0 ± 1.9 (0.0–8.5)	3.2 ± 2.4 (0.2–8.7)
GTV-70% – GTV-3D	–0.5 ± 1.2 (0.0–3.6)	1.5 ± 1.5 (0.0–4.6)	0.8 ± 2.3 (0.0–7.4)	3.0 ± 1.8 (0.2–8.8)
IGTV-10 – GTV-3D	–0.5 ± 0.9 (0.1–2.1)	1.0 ± 1.4 (0.1–3.8)	0.4 ± 1.9 (0.0–5.5)	2.4 ± 1.4 (0.3–6.2)

4D volume: GTV-0%, GTV-20%, GTV-50%, GTV-70% and IGTV-10; 3D volume: GTV-3D.

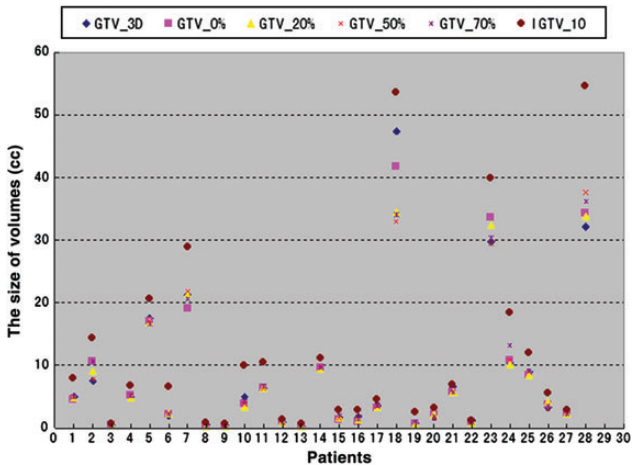

Fig. 4. The size of the volumes derived from the axial 3DCT and 4DCT for all the patients.

MI

The MIs of GTV-0 and GTV-3D, GTV-20% and GTV-3D, GTV-50% and GTV-3D, and GTV-70% and GTV-3D were 0.48 ± 0.21, 0.50 ± 0.21, 0.50 ± 0.23, and 0.48 ± 0.21, respectively. The variation in the MIs of GTV-0% and GTV-3D, GTV-20% and GTV-3D, GTV-50% and GTV-3D, and GTV-70% and GTV-3D was not significant ($F = 0.100$, $P = 0.960$). The MI of IGTV-10 and GTV-3D was 0.55 ± 0.17, which showed no significant correlation to the vector ($r = -0.284$, $P = 0.143$). Figure 6 shows the MI of the 4D volumes and the 3D volume.

DI

The DIs of GTV-3D in IGTV-10, and IGTV-10 in GTV-3D were 0.88 ± 0.14 and 0.59 ± 0.16, respectively,

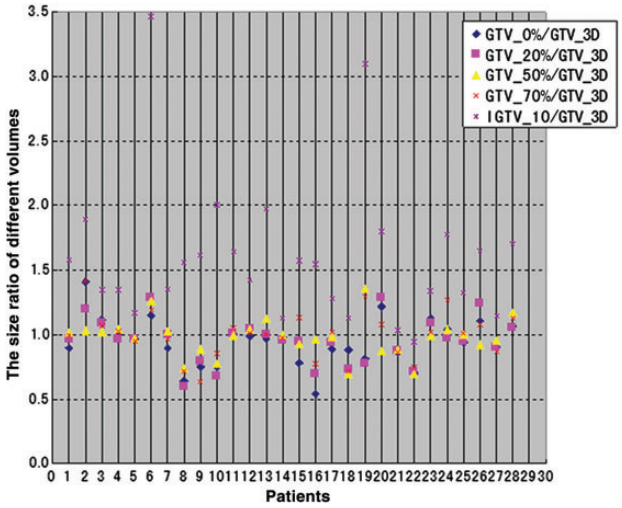

Fig. 5. The size ratios of GTV_0% to GTV_3D, GTV_20% to GTV_3D, GTV_50% to GTV_3D, GTV_90% to GTV_3D, and IGTV_10 to GTV_3D.

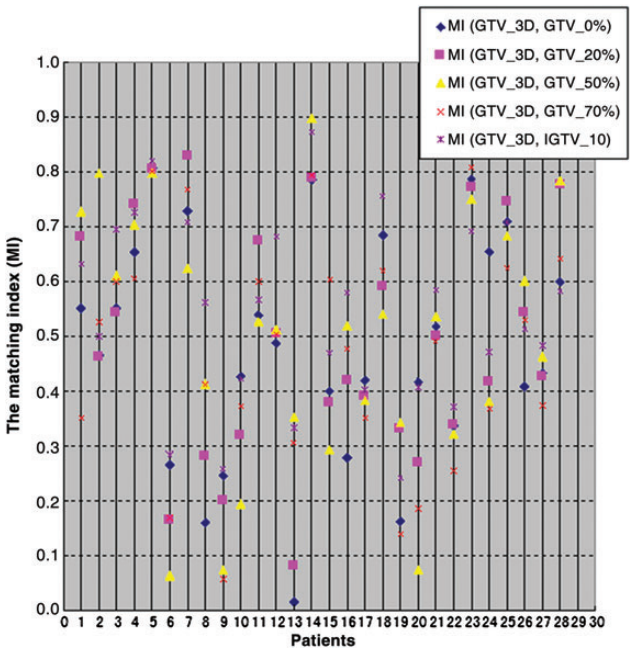

Fig. 6. The marching indices (MI) of GTV_0% and GTV_3D, GTV_20% and GTV_3D, GTV_50% and GTV_3D, GTV_90% and GTV_3D, and IGTV_10 and GTV_3D.

showing a significant difference ($t = 9.646$, $P < 0.001$). The DI of IGTV-10 in GTV-3D demonstrated a significant correlation to the vector ($r = -0.420$, $P = 0.026$), while the DI of GTV-3D in IGTV-10 showed no significant correlation to the vector ($r = 0.233$, $P = 0.233$). The median DI of IGTV-10 in GTV-3D for Group A and Group B were 0.65 and 0.54, respectively, with no significant difference ($z = -1.743$, $P = 0.082$).

DISCUSSION

Currently, 4DCT is widely used to estimate volumetric variations in target volumes throughout a respiratory cycle. The volumetric changes at different phases are mainly caused by residual motion artifacts during 4DCT imaging [3]. Nakamura *et al*. [20], determined the coefficient of variation (CV) of GTV sizes for all phases of 4DCT scans for 35 lung tumors, to have a mean of 3.92% (range, 0.54–8.99%). Rietzel *et al*. [7] reported the CV of GTV size in 4DCT scans for 10 lung tumors as 6.0 ± 3.0%. Our study indicated the CV was 8.76 ± 6.47%, which was similar to the result of Rietzel *et al.*, but greater than the result of Nakamura *et al*. Further analysis showed that the motion vector determined by Nakamura *et al.* was only 3.3 ± 1.9 mm, which was less than that found in our study (5.2 ± 3.5 mm), and also less than that reported by Rietzel *et al*. (7.7 ± 3.8 mm). Furthermore, our study showed the CV for Group A was greater than that for Group B ($P = 0.029$). These studies indicate that the tumor motion may contribute to increasing the volume variation between different phases because a tumor with larger motion amplitude is likely to produce more residual motion artifacts. In our study, however, no significant correlation was observed between the vector and the CV ($r = 0.372$, $P = 0.089$), which suggests that other factors might affect the CV for GTV sizes, such as partial volume effects in CT data, delineation errors, tumor deformation, and so on.

One of the important roles of 4DCT is assessing tumor motion so we can acquire population-based or site-specific tumor motion information to guide the expansion of ITVs based on 3DCT. Our premise was that 3DCT doesn't encompass much motion information, in other words, the size of GTV-3D is not significantly greater than that of the GTV from a single phase, otherwise the expansion would result in more normal tissue being unnecessarily irradiated. Our data supported the premise. The mean size ratios of the GTV from a single phase to GTV-3D were ~1. Fredberg Persson G *et al*. [21] also observed the size of the GTVs derived from the helical 3DCT, end-inspiration (Insp), end-expiration (Exp), and mid-ventilation (MidV) bins of the 4DCT scan. The median size ratios of GTV_{Insp} to GTV_{BH}, GTV_{Exp} to GTV_{3D}, and GTV_{MidV} to GTV_{3D} were 0.92, 1.00, and 1.05, respectively, i.e. similar to our results. Identifying the factors affecting tumor motion contributes to predicting tumor motion features. The location of a tumor is the main factor influencing the tumor motion. Tumor motion for the middle and lower lobe is significantly greater than for the upper lobe. In addition, our study showed a significant positive correlation between tumor size and tumor motion in the CC direction ($r = 0.395$, $P = 0.037$). However, we should not ignore the variation of tumor motion observed for a specific patient. The standard deviation of tumor motion in the 3D direction was 3.5 cm, while the mean

tumor motion was merely 5.2 cm, which indicates that patient-specific variation in tumor motion is large.

In our early study, we evaluated the centroid shifts of PTVs derived from 3DCT and all phases of 4DCT, and demonstrated the uncertainty of a target derived from 3DCT [17]. When estimating the centroid shifts of the GTV from a certain phase (GTV-0%, GTV-20%, GTV-50%, and GTV-70%) and GTV-3D, we found the mean centroid shifts were again very small. The small variation in centroid shifts of GTVs from different phases and GTV-3D indicates that respiration has little effect on centroid shifts ($P = 0.990$). The highly similar MIs of the GTV from different phases of the 4DCT and GTV-3D revealed a surprisingly consistent similarity of the GTV from different phases of the 4DCT and GTV-3D. It further demonstrates the uncertainty or randomness of the GTV derived from 3DCT. It is necessary to expand the internal margin isotropically using the population-based motion information for 3DCT-based treatment planning. In addition, our study indicated that tumor motion in the CC direction was significantly greater than for the LR ($P = 0.006$) or the AP ($P = 0.008$) directions for Group B, while the variations were not significant for Group A. Therefore, the greater margin should be used in the CC direction for tumors in the middle and lower lobe.

IGTV-10 encompasses the motion information for the tumor in the whole respiratory cycle [19]. Comparing volumetric difference between GTV-3D and IGTV-10 contributes to identifying the motion information encompassed by axial 3DCT. Our study showed that the size ratio of IGTV-10 to GTV-3D was 1.60 ± 0.55 (and the ratio of the median size of IGTV-10 to GTV-3D was 1.54), with a significant difference ($P = 0.001$). There was a positive correlation between the size ratio of IGTV-10 and GTV-3D and the vector ($r = 0.667$, $P < 0.001$). Bradley *et al*. [22] reported that the mGTV size based on MIP images of 4DCT was larger than the GTV based on helical CT images ($P = 0.001$), and the ratio of the median size of mGTV to GTV was 1.34, similar to our study. This suggests that the axial scanning mode doesn't increase the tumor motion included in the GTV for conventional 3DCT, compared to the helical scanning mode. In addition, our data showed the size ratio of GTV-3D to IGTV-10 was 0.75 ± 0.15 for Group A with a tumor motion vector of 3.2 ± 1.7 mm. Nevertheless, Nakamura *et al*. [20] reported that the size ratio of GTV ($TV_{slow\ CT}$) derived from slow CT to IGTV ($TV_{4D\ CT}$) derived from 4DCT was 0.75 ± 0.17 for tumors in the upper or middle lobes with a motion vector of 3.3 ± 1.9 mm. Such similar results demonstrate that the GTV derived from slow CT can't encompass more motion information than the GTV from axial 3DCT for tumors with a relatively small motion range.

Analyzing the inclusion relation between GTV-3D and IGTV-10, we found there was 12% of GTV-3D not included in IGTV-10 on average. It indicated IGTV-10 was unable to encompass GTV-3D completely. The variations in the breathing pattern may be the main cause of this result. A poorly reproducible breathing pattern can not only result in missing images at a certain respiratory phase for some table indices, leading to gaps in resorted 4DCT targets [3, 23], but also result in the target derived from random 3DCT breaking away from the range of IGTV-10. A recent study by Cai *et al*. [24] indicated that the gating window ITV could be underestimated by 4DCT due to respiration variations, and an additional margin was required to account for the potential error. Haasbeek *et al*. [25] reported that the difference in ITV position exceeded 5 mm in the 3D direction between coached and free breathing 4DCT scans only when the mobile tumor motion exceeded 10 mm, or 56%. However, we did not find a positive significant correlation between DI of GTV-3D in IGTV-10 and the motion vector ($P = 0.233$). Additionally, our study showed that 41% of IGTV-10 was not included in GTV-3D on average, and that the proportion increased as the tumor motion increased ($r = 0.420$, $P = 0.026$). This suggests that IGTV-10 encompasses much more respiration motion information than GTV-3D, especially for tumors with larger motion.

In this article, we verified the irregularity or randomness of 3DCT scanning phases. It is difficult to abandon the isotropic margin accounting for the tumor motion in 3DCT-based treatment planning. In other words, 4DCT-based radiotherapy is the development direction for individual therapy. However, a 4DCT scan is probably unable to account for the breathing state during treatment due to the variation in breathing pattern. In addition, a tumor with larger motion amplitude is likely to produce more residual motion artifacts. We need to realize the limitations of the 4DCT technique and continue work to improve it.

It should be noted that intra-observer target volume delineation error might reduce the accuracy of GTVs delineated on the 3DCT and 4DCT images [26], though all the delineation was performed by an observer. Manual delineating on each phase of 4DCT would consume lots of time. Automated 4DCT propagation tools could significantly decrease GTV delineating time, without significantly decreasing the inter- and intra- observer variability [27]. Additionally, it is impossible to avoid the impact of registration error on the comparison of MI or DI between GTV-3D and 4D targets. Slight registration error may change the results greatly for some small tumors. Comparison of 3D with 4D scanning depends heavily on the scan protocols used. If the scan parameters are changed, different results may be obtained.

CONCLUSION

On the whole, the difference in GTV size between axial 3DCT and a certain phase of 4DCT was not significant. The tumor motion measured by 4DCT can be used in

CTV-to-ITV expansion based 3DCT, but the expansion should be isotropic due to the randomness of 3DCT. The respiration motion information included in 4DCT is far larger than in 3DCT, and the gap increases as the tumor motion increases. The IGTV derived from 4DCT can't include the GTV from 3DCT completely due to respiration variations. An additional margin may be required to account for the potential error when defining the ITV based on a 4DCT scan.

FUNDING

This research was supported in part by Science and Technology Development Project of Shandong Province of China (2012GSF11839), Natural Science Foundation of Shandong Province of China (ZR2011HM004), Science Foundation for Youth of Shandong Academy of Medical Science of China (2012-21).

REFERENCES

1. Li G, Citrin D, Camphausen K *et al*. Advances in 4D medical imaging and 4D radiation therapy. *Technol Cancer Res Treat* 2008;**7**:67–81.
2. Chen GT, Kung JH, Beaudette KP *et al*. Artifacts in computed tomography scanning of moving objects. *Geriatr Nephrol Urol* 2004;**14**:19–26.
3. Rietzel E, Pan T, Chen GT *et al*. Four-dimensional computed tomography: image formation and clinical protocol. *Med Phys* 2005;**32**:874–89.
4. Balter JM, Lam KL, McGinn CJ *et al*. Improvement of CT-based treatment planning model of abdominal targets using static exhale imaging. *Int J Radiat Oncol Biol Phys* 1998;**41**:939–43.
5. Wagman R, Yorke E, Giraud P *et al*. Reproducibility of organ position with respiratory gating for liver tumors: use in dose-escalation. *Int J Radiat Oncol Biol Phys* 2003;**55**:659–68.
6. Wong JW, Sharpe MB, Jaffray DA *et al*. The use of active breathing control (ABC) to reduce margin for breathing motion. *Int J Radiat Oncol Biol Phys* 1999;**44**:911–9.
7. Rietzel E, Liu AK, Doppke KP *et al*. Design of 4D treatment planning target volumes. *Int J Radiat Oncol Biol Phys* 2006;**66**:775–80.
8. Lagerwaard FJ, Van Sornsen de Koste JR, Nijssen-Visser MRJ *et al*. Multiple "slow" CT scans for incorporating lung tumor mobility in radiotherapy planning. *Int J Radiat Oncol Biol Phys* 2001;**51**:932–7.
9. Lewis JH, Jiang SB. A theoretical model for respiratory motion artifacts in free-breathing CT scans. *Phys Med Biol* 2009;**54**:745–55.
10. Tachibana M. Total breathing phase scan (slow scan) method in the free breathing state by multi-detector-row computed tomography scanner in radiotherapy planning. *Nippon Hoshasen Gijutsu Gakkai Zasshi* 2008;**64**:297–305.
11. Gagne IM, Robinson DM. The impact of tumor motion upon CT image integrity and target delineation. *Med Phys* 2004;**31**:3378–92.
12. Dinkel J, Welzel T, Bolte H *et al*. Four-dimensional multislice helical CT of the lung: qualitative comparison of retrospectively gated and static images in an *ex-vivo* system. *Radiother Oncol* 2007;**85**:215–22.
13. Underberg RW, Lagerwaard FJ, Cuijpers JP *et al*. Four-dimensional CT scans for treatment planning in stereotactic radiotherapy for stage I lung cancer. *Int J Radiat Oncol Biol Phys* 2004;**60**:1283–90.
14. Guckenberger M, Wilbert J, Meyer J *et al*. Is a single respiratory correlated 4D-CT study sufficient for evaluation of breathing motion? *Int J Radiat Oncol Biol Phys* 2007;**67**:1352–9.
15. Hof H, Rhern B, Haering P *et al*.. 4D-CT-based target volume definition in stereotactic radiotherapy of lung tumours: comparison with a conventional technique using individual margins. *Radiother Oncol* 2009;**93**:419–23.
16. Wang L, Hayes S, Paskalev K *et al*. Dosimetric comparison of stereotactic body radiotherapy using 4D CT and multiphase CT images for treatment planning of lung cancer: evaluation of the impact on daily dose coverage. *Radiother Oncol* 2009;**91**:314–24.
17. Li FX, Li JB, Zhang YJ *et al*. Comparison of the planning target volume based on three-dimensional CT and four-dimensional CT images of non-small-cell lung cancer. *Radiother Oncol* 2011;**99**:176–80.
18. Giraud P. Influence of CT images visualization parameters for target volume delineation in lung cancer. *Radiother Oncol* 2000;**56**(Suppl 1):39.
19. Ezhil M, Vedam S, Balter P *et al.* Determination of patient-specific internal gross tumor volumes for lung cancer using four-dimensional computed tomography. *Radiat Oncol* 2009;**4**:4.
20. Nakamura M, Narita Y, Matsuo Y *et al*. Geometrical differences in target volumes between slow CT and 4D CT imaging in stereotactic body radiotherapy for lung tumors in the upper and middle lobe. *Med Phys* 2008;**35**:4142–8.
21. Fredberg Persson G, Nygaard DE, Munck Af Rosenschöld P *et al*. Artifacts in conventional computed tomography (CT) and free breathing four-dimensional CT induce uncertainty in gross tumor volume determination. *Int J Radiat Oncol Biol Phys* 2011;**80**:1573–80.
22. Bradley JD, Nofal AN, El Naqa IM *et al*. Comparison of helical, maximum intensity projection (MIP), and averaged intensity (AI) 4D CT imaging for stereotactic body radiation therapy (SBRT) planning in lung cancer. *Radiother Oncol* 2006;**81**:264–8.
23. Keall P. 4-dimensional computed tomography imaging and treatment planning. *Semin Radiat Oncol* 2004;**14**:81–90.
24. Cai J, McLawhorn R, Read PW *et al*. Effects of breathing variation on gating window internal target volume in respiratory gated radiation therapy. *Med Phys* 2010;**37**:3927–34.
25. Haasbeek CJ, Spoelstra FO, Lagerwaard FJ *et al*. Impact of audio-coaching on the position of lung tumors. *Int J Radiat Oncol Biol Phys* 2008;**71**:1118–23.
26. Louie AV, Rodrigues G, Olsthoorn J *et al*. Inter-observer and intra-observer reliability for lung cancer target volume delineation in the 4DCT era. *Radiother Oncol* 2010;**95**:166–71.
27. Gaede S, Olsthoorn J, Louie AV *et al*. An evaluation of an automated 4D-CT contour propagation tool to define an internal gross tumour volume for lung cancer radiotherapy. *Radiother Oncol* 2011;**101**:322–8.